113, 42-54 (1977)

# COHERENT OPTICAL SPECTROSCOPY OF MOLECULES AND MOLECULAR BEAMS

A. H. Zewail, D. E. Godar, K. E. Jones, T. E. Orlowski, R. R. Shah, and A. Nichols
Arthur Amos Noyes Laboratory of Chemical Physics, California Institute of Technology
Pasadena, California 91125

## Abstract

This paper presents our recent work on coherent optical spectroscopy of molecules and molecular beams. The theory for these nonlinear optical effects is summarized and related to the measurements in the gas phase and in the condensed phase. Finally, we discuss the importance of these methods, which disentangle the inhomogeneous optical resonances, in understanding nonradiative and optical dephasing processes.

## Why Coherent Optical Spectroscopy ?

In conventional optical techniques the molecular ensemble is excited in a way such that the excited state population density can be at most half that of the total population density. This incoherent coupling between the molecules and the radiation field gives rise to the following upper state population at any time t:

$$N_a(t) = \left(\frac{NBD}{A+2BD}\right) [1 - \exp -(A + 2BD)t] \quad (1)$$

where D is the energy density of light turned on at t = 0 when the molecules are in their ground state, N is the total number of molecules, and A and B are the well-known Einstein coefficients.

If all the molecules are the same (homogeneous environment) then when the light is turned off

$$N_a(t) = N_a^o e^{-At} = N_a^o e^{-t/\tau} \quad (2)$$

where $\tau$ is the lifetime of the upper state and $N_a^o$ is the steady state population. This shutter experiment is, of course, what every spectroscopist can do to measure $\tau$ directly.

Quantum mechanically, one arrives at the same conclusion by using the Wigner-Weisskopf approximation[1] or by quantizing the radiation field .[2] Knowing that the upper state has a finite lifetime, the Fourier transform of the emission probability function will give a Lorentzian resonance that can perhaps be measured in the laboratory. One might therefore conclude that careful measurements of the linewidth of optical transitions will give the dynamics of molecular excited levels. Unfortunately, these molecules are not isolated from the rest of the ensemble which may or may not be "homogeneous".

In gases, there are different eigenpackets (i.e., the distribution of molecular states that are homogeneous) which form an inhomogeneous resonance. The Doppler resonance is therefore a weighted statistical distribution for the population among all packets. To characterize the dynamics one must therefore know the actual width of the homogeneous packets as well as the relative importance of pressure induced broadening (caused by collision-induced phase interruptions) and pressure induced velocity changes during the optical pumping.

In solids, although the sites are not "moving", the problem is similar because "Doppler solids" do exist. In other words, different molecules (or ions) experience different crystal fields and thus are located at slightly shifted energies which appear in the frame of the on-resonance transition as being moving. Equivalently one says that the crystal ensemble is "inhomogeneous".

In molecular beams, although there is no collisional broadening, intramolecular relaxation processes can destroy the phase coherence of the ground-excited system and may cause the homogeneous width of the resonance to be different from the width due to spontaneous emission.

With the advances in laser technology, spectroscopists have tried to narrow these inhomogeneous optical resonances using different methods. All these methods extract a linewidth that is smaller than the inhomogeneous width. However, the contribution of the different coherent and incoherent decay processes cannot be extracted in a straightforward manner.

This paper will focus on the importance of coherent optical spectroscopy in studying molecular dynamics in gases, solids and molecular beams. These techniques are capable of disentangling the inhomogeneous resonances and give information about the nature of homogeneous packets hidden under the inhomogeneous transitions. Furthermore, it allows one to directly measure both optical $T_1$ and $T_2$, thus giving information about spontaneous radiative and nonradiative processes, and about the origin of vibronic dephasing in the

excited ensembles. The questions we have in mind are:

1. What are the radiative and nonradiative decays (optical $T_1$ processes) that contribute to the width of the resonance?
2. Are excited electronic states coherent?
3. Why do excited states lose their phase coherence ($T_2$ processes)?
4. Is there any energy threshold for the dephasing processes?
5. Does intramolecular relaxation lead into a dephasing process even at zero pressure (molecular beams)?
6. What is the role of excited state preparation on the coherent and incoherent time evolution of the system?

## Theory of Coherent Optical Effects

Our interest at Caltech has focussed on the problem of measuring coherence effects via laser spectroscopy as a means of probing inter- and intramolecular dephasing processes and their contributions to the observed linewidths and lifetimes of (electronic) molecular states. This problem may be restated as an attempt to monitor the off-diagonal elements of the (mixed-case) density matrix describing the group of molecular resonances under observation. In particular, one is concerned with measuring the time-decay of these components as a result of the various dephasing processes (e.g., collisions in gases, lattice interactions in solids, intramolecular congested level structure in large molecules, etc.). As is well-known,[2] these off-diagonal elements are related to the macroscopic transverse polarization (or, alternatively, Dicke's "cooperation number"[3]) induced in the sample by forming a coherent superposition of the ground and excited states. This, in turn, is proportional to the amplitude of coherent (superradiant) emission in the direction of the incident radiation.

In a single molecule with a zero-order Hamiltonian (3), the wavefunction at any time may be written as a linear combination (4). If the states $|a\rangle$ and $|b\rangle$ are coupled by the radiation field, a dipole moment, oscillating at the transition frequency $\omega_o$, will be formed (5) as a result of the superposition of states:

$$\mathcal{H}_o|a\rangle = \frac{\hbar\omega_o}{2}|a\rangle \qquad \mathcal{H}_o|b\rangle = -\frac{\hbar\omega_o}{2}|b\rangle \qquad \mathcal{H}_o = \frac{\hbar\omega_o}{2}\sigma_3 \tag{3}$$

$$\Psi(t) = a(t)e^{-i\frac{\omega_o}{2}t}|a\rangle + b(t)e^{i\frac{\omega_o}{2}t}|b\rangle \tag{4}$$

$$\langle\Psi(t)|\hat{\mu}|\Psi(t)\rangle = ab^*\,\mu_{ba}\,e^{-i\omega_o t} + ba^*\,\mu_{ab}\,e^{i\omega_o t} \tag{5}$$

where $\sigma_3$ is the Pauli matrix and $\mu_{ab}$ is assumed to be real, i.e., $\mu_{ab} = \mu_{ba} \equiv \mu$. We define $\rho_{RF}$ as the density matrix in the "rotating frame" (at frequency $\omega$) which is related to the laboratory density matrix $\rho'$ by the transformation in equation (6), allowing us to write the macroscopic polarization $\vec{P}$ for "thin" samples as in (7):

$$\rho_{RF} = \underset{\approx}{U}^{-1}\rho'\underset{\approx}{U} = e^{i\omega\sigma_3 t/2}\begin{pmatrix}\langle aa^*\rangle & \langle ab^*e^{-i\omega_o t}\rangle \\ \langle c.c.\rangle & \langle bb^*\rangle\end{pmatrix}e^{-i\omega\sigma_3 t/2}$$

$$= \begin{pmatrix}\langle aa^*\rangle & \langle ab^*e^{-i\Delta t}\rangle \\ \langle c.c.\rangle & \langle bb^*\rangle\end{pmatrix} = \begin{pmatrix}\rho_{aa} & \rho_{ab} \\ \rho_{ba} & \rho_{bb}\end{pmatrix} \equiv \rho \tag{6}$$

$$P = N\,\mu(\rho_{ab}\,e^{-i\omega t} + \rho_{ba}\,e^{i\omega t}) \qquad \text{and} \qquad \omega + \Delta = \omega_o \quad . \tag{7}$$

Here the brackets indicate an N-molecule ensemble averaged over the indicated density matrix elements of the individual molecules, which may have different $\omega_o$'s, and hence different $\Delta$'s. As shown by Feynman, Vernon and Hellworth (FVH[4] picture) the off-diagonal elements of $\rho$ are related to the components of the so-called r vector in the following way:

$$\begin{pmatrix}r_1 \\ r_2 \\ r_3\end{pmatrix} = \begin{pmatrix}\rho_{ab} + \rho_{ba} \\ i(\rho_{ab} - \rho_{ba}) \\ \rho_{aa} - \rho_{bb}\end{pmatrix} \quad . \tag{8}$$

The significance of the r vector is that its cross product with an effective field $E_{eff}$ gives a torque equation analogous to that used in magnetic resonance[5] spectroscopy, i.e.,

$$\dot{\vec{r}} = \vec{E}_{eff} \times \vec{r} \tag{9}$$

where $$\vec{E}_{eff} = (-\mu \mathcal{E}/\hbar,\ 0,\ \Delta) \quad . \tag{10}$$

The induced polarization is therefore related only to $r_1$ and $r_2$ since by equations (7) and (8)

$$P = \frac{N\mu}{2}(r_1 - ir_2)e^{-i\omega t} + \frac{N\mu}{2}(r_1 + ir_2)e^{i\omega t} \quad . \tag{11}$$

This polarization acts as a source term in the following Maxwell's equation (in MKS units) to form a "signal" field $E_S$

$$\vec{\nabla} \times \vec{\nabla} \times \vec{E}_S + \mu_0 \sigma \dot{\vec{E}}_S + \mu_0 \epsilon_0 \ddot{\vec{E}}_S = -\mu_0 \ddot{\vec{P}} \quad . \tag{12}$$

If the field $\vec{E}_S$ and polarization $\vec{P}$ are assumed to take the following form, where $\mathcal{E}$ and $\mathcal{P}$ are slowly varying

$$E_S(z, t) = \tfrac{1}{2}\, \mathcal{E}_S(z, t)\, e^{-i(\omega t - kz)} + c.c. \tag{13}$$

$$P(z, t) = \tfrac{1}{2}\, \mathcal{P}(z, t)\, e^{-i(\omega t - kz)} + c.c. \tag{14}$$

envelopes (SVEA)[2] in z and t over an optical wavelength or cycle, equation (12) becomes

$$\frac{\partial \mathcal{E}_S}{\partial z} + \frac{1}{c}\dot{\mathcal{E}}_S + \kappa \mathcal{E}_S = \frac{-i\omega}{2c\epsilon_0}\mathcal{P} \quad . \tag{15}$$

Ignoring $\kappa = \sigma/2c\epsilon_0$, the loss per unit length, and considering typical experimental conditions where $\partial \mathcal{E}_S/\partial z \gg (1/c)(\partial \mathcal{E}_S/\partial t)$, the following equation may be integrated over the length of the cell L to give

$$\mathcal{E}_S \cong \frac{-i\omega L}{2c\epsilon_0}\mathcal{P} \quad . \tag{16}$$

The fact that a radiation field can induce a macroscopic polarization that oscillates in time depending on $\mu$, $\mathcal{E}$ and $\Delta$, and damps by $T_1$ and $T_2$, has led to a variety of experiments for the observation of coherent optical transients (nutation, free induction decay, photon echoes) in solids, gases and more recently in molecular beams.[6] The experiments were performed using pulsed[7] or cw[8] laser techniques. Optical $T_2$ measurements together with measurements of spontaneous emission lifetime, which monitors the decay of the diagonal elements of the density matrix, have lead to a characterization of the decay processes of the two states selected by the laser. The solutions to these two-level problems are well-known in the literature and in several texts, and only a brief discussion is in order.

## Emission Detection of Optical Coherence[9, 10]

Recently we have developed a technique for the measurement of optical coherence in a variety of systems by monitoring the incoherent emission. This method is based on the notion that if the off-diagonal elements of the density matrix (representing a polarization) can be converted at a given time into a change in the diagonal elements (population) there will be a measurable alteration of the spontaneous emission. In this way, the coherence of the system can be monitored by measuring the right-angle resonance emission, giving a much smaller background signal. Simple considerations indicate that a $\pi/2$ pulse has this property of quantitatively converting the in-plane (transverse) polarization (in the FVH picture) to a population by rotating the vector r from the $r_2$ axis to the $r_3$ (population) axis. Thus an echo experiment may be represented pictorally as in Figure 1.

From these general considerations, one can see that in this picture, the spontaneous emission from a group of N molecules should start at zero (a), rise to a value of approximately $(N/2)\,[T_1^{(r)}]^{-1}$ (i.e., half the population times the radiative rate constant (b)), and fall slowly as the excited population is depleted. If, as the echo maximum is reached, a $\pi/2$ probe pulse is applied, the polarization will be converted into ground state population, and the emission will drop to zero. Further, the total integrated emission (over $4\pi$ sterradians and $t \to \infty$) without the probe pulse will be $\approx N/2$ photons, and with the probe pulse $\approx 0$.

The Hamiltonian for the system can be written as the sum of the zero-order Hamiltonian (3) and an interaction term representing the coupling of the two molecular states by the field:

$$\mathcal{H} = \frac{\hbar\omega_0}{2}\sigma_3 - \mu \cdot \mathcal{E}\, \sigma_1 \cos \omega t \tag{17}$$

where $\sigma_1$ is the Pauli matrix $\begin{pmatrix} 0 & 1 \\ 1 & 0 \end{pmatrix}$. The equation of motion is therefore given by

$$i\hbar \dot{\rho}' = [\mathcal{H}, \rho'] \quad . \tag{18}$$

Using equation (6) (i.e., $\rho' = \underset{\approx}{U}\, \rho\, \underset{\approx}{U}^{-1}$), one obtains the following equations for the Hamiltonian in the rotating frame:

$$\begin{aligned} i\hbar \dot{\rho} &= [\mathcal{H}_r, \rho] \\ \mathcal{H}_r &= \underset{\approx}{U}^{-1} \mathcal{H}\, \underset{\approx}{U} - \frac{\hbar\omega}{2}\sigma_3 \\ &= \frac{\hbar\Delta}{2}\sigma_3 - \mu\cdot\mathcal{E}\, e^{i\omega\sigma_3 t/2}\, \sigma_1\, e^{-i\omega\sigma_3 t/2} \cos\omega t \\ &\simeq \frac{\hbar\Delta}{2}\sigma_3 - \frac{\mu\cdot\mathcal{E}}{2}\sigma_1 \quad . \end{aligned} \tag{19}$$

The last step in equation (19) was done by using the following identity and ignoring terms that oscillate at twice the frequency $\omega$:

$$e^{i\omega\sigma_3 t/2}\, \sigma_1\, e^{-i\omega\sigma_3 t/2} = \sigma_1 \cos\omega t - \sigma_2 \sin\omega t \quad . \tag{20}$$

Given this time-independent Hamiltonian (19), one can solve for the time evolution of the density matrix in the rotating frame, which is

$$\rho(t) = e^{-i\mathcal{H}_r t/\hbar}\, \rho(0)\, e^{i\mathcal{H}_r t/\hbar} \equiv \underset{\approx}{S}^{-1} \rho(0)\, \underset{\approx}{S} \tag{21}$$

where $\underset{\approx}{S}$ is given by

$$\underset{\approx}{S} = \begin{bmatrix} \cos\frac{\Omega}{2}t + i\frac{\Delta}{\Omega}\sin\frac{\Omega}{2}t & -i\frac{\omega_R}{\Omega}\sin\frac{\Omega}{2}t \\ -i\frac{\omega_R}{\Omega}\sin\frac{\Omega}{2}t & \cos\frac{\Omega}{2}t - i\frac{\Delta}{\Omega}\sin\frac{\Omega}{2}t \end{bmatrix} \quad . \tag{22}$$

The Rabi frequency is $\omega_R$, and $\Omega = (\omega_R^2 + \Delta^2)^{\frac{1}{2}}$.

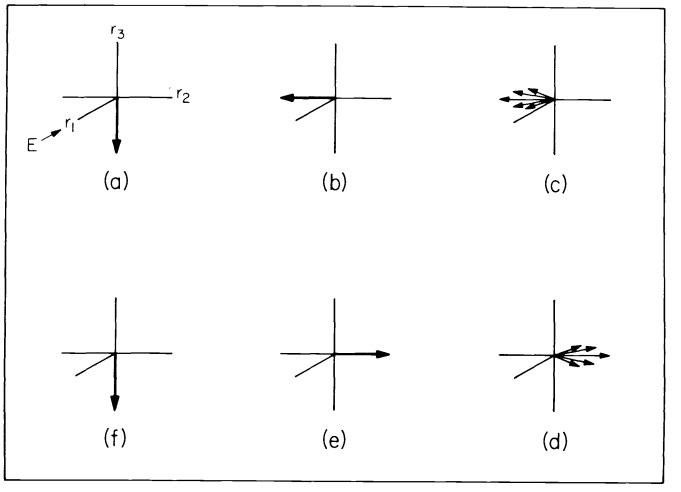


Fig. 1. A schematic for the description of the right-angle photon echo: (a) all the molecules are in the ground state; (b) after a $\pi/2$ pulse; (c) inhomogeneous dephasing; (d) after a $\pi$ pulse; (e) the echo; (f) storage of the echo in the ground state (i.e., termination of the spontaneous emission from the upper level).

The experiment may now be simulated as follows. Consider a group of molecules having different transition frequencies $\omega_0$ and centered around $\omega$. At t = 0 these molecules are all in the ground state when the laser is switched into resonance (at $\omega$). For a $\pi/2$ pulse ($\Delta = 0$, $\omega_R t = \pi/2$) the system evolves in time

from $\rho(0) = \begin{pmatrix} 0 & 0 \\ 0 & 1 \end{pmatrix}$ to

$$\rho_{\pi/2} = \underset{\approx}{S}^{-1}_{\pi/2}\, \rho(0)\, \underset{\approx}{S}_{\pi/2} = \tfrac{1}{2}\begin{pmatrix} 1 & i \\ -i & 1 \end{pmatrix} \quad . \tag{23}$$

The laser is then switched off for a period of time $\tau_1$. During this time, several processes must be accounted for. First, the different molecules spanned by the effective width of the laser (i.e., the intrinsic width and the power broadening of the transition, for a Lorentzian resonance, the FWHM = $2\theta$ centered at $\omega$) will get out-of-phase with each other. A homogeneous packet at frequency $\omega_o = \omega + \delta$ will then precess in the rotating frame at a frequency $\delta$, i.e.,

$$\rho^{(1)}(\tau_1) = \underset{\approx}{S}^{-1}_{\tau_1}\, \rho(\pi/2)\, \underset{\approx}{S}_{\tau_1} \tag{24}$$

Explicitly, equation (24) gives

$$\rho^{(1)}(\tau_1) = \tfrac{1}{2}\begin{pmatrix} 1 & ie^{-i\delta\tau_1} \\ -ie^{+i\delta\tau_1} & 1 \end{pmatrix} \tag{25}$$

since

$$\underset{\approx}{S}_{\tau_1} = \begin{pmatrix} e^{i\delta t/2} & 0 \\ 0 & e^{-i\delta t/2} \end{pmatrix} \quad . \tag{26}$$

Second, decay processes ($T_1$ and $T_2$) must also be taken into account. If $T_{1a}$ and $T_{1b}$ are, respectively, the lifetimes of the excited and ground states and $T_2'$ is the pure dephasing term, then (25) becomes:

$$\rho^{(2)}(\tau_1) = \tfrac{1}{2}\begin{pmatrix} e^{-\tau_1/T_{1a}} & ie^{-i\delta\tau_1}e^{-\tau_1/T_2} \\ -ie^{+i\delta\tau_1}e^{-\tau_1/T_2} & e^{-\tau_1/T_{1b}} \end{pmatrix} \equiv \rho(\tau_1) \tag{27}$$

where

$$\frac{1}{T_2} = \frac{1}{2}\left(\frac{1}{T_{1a}} + \frac{1}{T_{1b}}\right) + \frac{1}{T_2'} \quad . \tag{28}$$

At $t = \tau_1$, the laser is switched back to frequency $\omega$ for a $\pi$-pulse ($\Delta = 0$, $\omega_R t = \pi$), the result being indicated in (29) Switching back off-resonance for a time $\tau_2$, and using the previous considerations, the density matrix at $t = (\tau_1 + \tau_2)$ is given in (30).

$$\rho(\tau_1, \pi) = \underset{\approx}{S}^{-1}_{\pi}\, \rho(\tau_1)\, \underset{\approx}{S}_{\pi} = \tfrac{1}{2}\begin{pmatrix} e^{-\tau_1/T_{1b}} & -ie^{+i\delta\tau_1}e^{-\tau_1/T_2} \\ \text{c.c.} & e^{-\tau_1/T_{1a}} \end{pmatrix} \tag{29}$$

$$\rho(\tau_1+\tau_2) = \tfrac{1}{2}\begin{pmatrix} e^{-\tau_1/T_{1b}}e^{-\tau_2/T_{1a}} & -ie^{-i\delta(\tau_2-\tau_1)}e^{-(\tau_1+\tau_2)/T_2} \\ ie^{+i\delta(\tau_2-\tau_1)}e^{-(\tau_1+\tau_2)/T_2} & e^{-\tau_1/T_{1a}}e^{-\tau_2/T_{1b}} \end{pmatrix} \tag{30}$$

The 'probe' $\pi/2$ pulse is now applied by switching the laser again to frequency $\omega$. Looking only at $\rho_{aa}$ (since the spontaneous emission is determined by this term), we get the result (31). This is averaged over the (previously mentioned) Lorentzian distribution of $\delta$'s to give (32).

$$2\,\rho_{aa} = \tfrac{1}{2}\left(e^{-\tau_1/T_{1b}}e^{-\tau_2/T_{1a}} + e^{-\tau_1/T_{1a}}e^{-\tau_2/T_{1b}}\right) - e^{-(\tau_1+\tau_2)/T_2}\cos\delta(\tau_2\ \tau_1) \tag{31}$$

$$2\langle\rho_{aa}\rangle = \tfrac{1}{2}\left(e^{-\tau_1/T_{1b}}e^{-\tau_2/T_{1a}} + e^{-\tau_1/T_{1a}}e^{-\tau_2/T_{1b}}\right) - e^{-(\tau_1+\tau_2)/T_2}\,e^{-|\tau_2-\tau_1|\theta} \quad . \tag{32}$$

The echo may be measured by looking at the difference in emission before and after the pulse, which would be proportional to the difference of $\rho_{aa}$ from (30) and (32) One notices that other than the second term in (32), which gives a sloping baseline, the echo signal, I, for fixed $\tau_1$ and varying $\tau_2$ is

$$I(\tau_2) = -A\, e^{-(\tau_1+\tau_2)/T_2}\, e^{-|\tau_2-\tau_1|\theta} \tag{33}$$

where A is a constant. This result can also be obtained if the emission resulting from the pulse sequence (characterized by different $\rho_{aa}$'s for the on and off pulse periods) is integrated over all time. It should be mentioned that expression (33) is for the case where the laser is turned off during $\tau_1$ and $\tau_2$ periods. However, our earlier experiments[10] were done by frequency switching which resulted in the modulation of the echo shape at the switching frequency. A full account of this treatment will be published later.[11] Similar expressions for the free induction decay (FID), the optical nutation, and the incoherent resonance decay (IRD) can be obtained.

## Experimental

### The Right-Angles Coherent Transients[9, 10]

In these experiments, an intense single mode tunable dye laser was used for the excitation. An $Ar^+$ ion laser (Spectra Physics Model 170) was used to pump a free jet stream dye laser. A modified Spectra Physics (Model 580 A) dye laser was used so a single mode could be switched out of the transition resonance frequency by an electro-optic element.[8] Special attention was given to the alignment procedure so the dispersion of the crystal in the electric field was caused by the modulation of the refractive index along a principal axis of the dielectric ellipsoid. The modulation is done transversely and is different from the switching procedure of Telle and Tang[12] used for very rapid tuning of cw dye lasers. From the frequency spectrum and the heterodyne pattern we obtained an electro-optic dispersion for the AD*P crystal of 0.6 Mhz/V. The net laser power of the single mode can be varied up to 90 mW and the field is linearly polarized.

The single mode beam was split so both the frequency of the transition and the "quality" of the single mode could be checked during the experiments. The single-mode spectrum was monitored with a Fabry-Perot interferometer that is scanned to allow the observation of on-resonance and off-resonance mode structure of the laser beam. Most of the laser beam intensity was used in the forward direction for the excitation of the sample. For the study of low pressure gases, a sample tube with Brewster-angle optical windows was used. A cold finger at the side of the tube was used to control the pressure of the gas. For solid state experiments, the crystal was oriented in a liquid helium Dewar that could be pumped to temperatures below the λ-point. For beam experiments, the laser was focussed on a spot near the slit of the beam apparatus, as shown schematically in Figure 2.

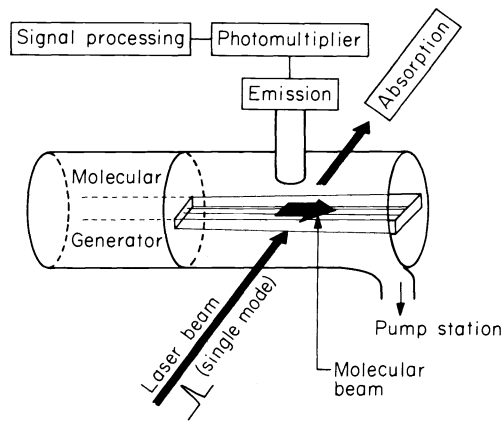


Fig. 2. A schematic for the crossed molecular and laser beams for the studies of coherent transients at zero pressure.

The emission was collimated at a right angle to the exciting beam and focussed on a cooled photomultiplier (EMI-9558). The photomultiplier was magnetically and electrostatically shielded. Since noise will be introduced because of the laser light scattering, a sharp cutoff glass filter and/or a 0.5 m Jarrell Ash spectrometer was placed in front of the phototube. The output of the photomultiplier was terminated in a boxcar integrator (PAR Model 162) or a sampling scope (Tektronics Model 1S1). The

photomultiplier was coupled AC into the boxcar and the output was traced on an X-Y recorder.

The Forward Coherent Transient Experiments[8]

In these experiments we monitored the laser intensity in the forward direction. Carefully mounted photodiodes were used in combination with filters to obtain the transients. These transients appear either as a coherent absorption and emission, as in the optical nutation, or as beating with the incident beam, as in the free induction decay signal. The output of the biased diode was amplified and fed into either an oscilloscope or the boxcar integrator. The laser power was measured by a Spectra Physics power meter (Model 401 B). Knowing the power of the single mode and the beam diameter gave the radiation density at the sample.

## Optical Coherence of Two- and Many-Level Molecules

Consider a molecule with a state $|s\rangle$ (i.e., $|s\rangle \equiv \phi_s$ is the $|a\rangle$ state in the previous formalism) that carries most of the oscillator strength from the ground state $|0\rangle$, and that is imbedded in a manifold of $\{\ell\}$ states. The $\{\ell\}$ states (triplet or hot singlet levels) essentially do not couple radiatively to the ground state. If there were no intramolecular interactions, $v_{s\ell}$, the states are characterized by $T_1$ and $T_2$. These decay times represent the dephasing times of the levels ($T_2$'s) and the spontaneous decay times ($T_1$'s) which contain the radiative and nonradiative (say, the coupling to hot vibrational levels of the ground state) contributions:

$$\frac{1}{T_1} = \frac{1}{T_1^{(r)}} + \frac{1}{T_1^{(nr)}}$$

$$\frac{1}{T_2} = \frac{1}{T_2'} + \frac{1}{T_1} \quad . \tag{34}$$

The total dephasing time contains both the pure dephasing term and the spontaneous loss for the levels involved. Under these conditions, the electric field of the laser couples with the transition moment of the Born-Oppenheimer (BO) states,[13] $\mu_{os}$, thus recovering the classical two-by-two Rabi limit:

$$\underset{\approx}{\rho} = \begin{array}{c} \begin{array}{ccc} |0\rangle & |s\rangle & \{\ell\} \end{array} \\ \left( \begin{array}{ccc} |c_o|^2 e^{-t/T_{1o}} & c_o c_s^* e^{-i\Delta E_{os} t} e^{-\frac{1}{2}\left(\frac{1}{T_{1o}} + \frac{1}{T_{1s}}\right)t} e^{-t/T_2'} & 0 \\ c.c. & |c_s|^2 e^{-t/T_{1s}} & 0 \\ 0 & 0 & 0 \end{array} \right) \end{array} \tag{35}$$

where $\rho$ is the density matrix and $|c_i|^2$ is the probability of finding the system in state $|i\rangle$. Note that the diagonal elements are the same as those derived by the effective Hamiltonian method[14] for isolated molecules with no correlation among the decay channels, e.g.,

$$E_s = \epsilon_s - i/2 \frac{1}{T_1^r} - i/2 \frac{1}{T_1^{nr}} \quad . \tag{36}$$

Therefore in this no coupling limit the system decays by $T_1$ and dephases by $T_2'$ of the ground and excited ensemble.

Turning $v_{s\ell}$ on produces the true eigenstates which diagonalize the molecular Hamiltonian:[15]

$$\psi_m = \alpha_{ms} |s\rangle + \beta_{m\ell} \{|\ell\rangle\} \quad . \tag{37}$$

Now, if we prepare[16] the $\psi_m$'s states, we have the same situation as before. The difference, however, will be the change in the transition moment which is now smaller due to the dilution of $\mu_s$ among the effective $\{\ell\}$ manifold. Therefore, one expects the Rabi frequency to change to

$$\omega_R^{(m)} = (\alpha_{ms}\mu_{os} + \beta_{m\ell}\mu_{o\ell}) \cdot \mathcal{E}/\hbar \quad . \tag{38}$$

The density matrix contains the information about all the levels involved in the coupling and the exact time evolution of it is given by:

$$i\hbar \frac{\partial}{\partial t} \rho' = [(\mathcal{H}_{BO} + v(s|\ell) - \mu \cdot \mathcal{E} \cos \omega t),\ \rho'] - i\mathcal{R} \cdot \rho' \tag{39}$$

where $\mathcal{R}$ is Redfield's superoperator[17] and contains the $T_1$ and $T_2$ terms. The intermolecular dephasing of the true molecular eigenstates (TME) can therefore be handled if we assume a large phonon reservoir in solids[18] or a large reservoir of optically inactive molecules in gases.[19] As pointed out before, the total rate of dephasing at any temperature T in a solid is given by[18] where $|0\rangle$ and $|m\rangle$ are the two states

$$\Gamma_{total}(T) = \tfrac{1}{2}\left(\frac{1}{T_{1m}} + \frac{1}{T_{10}}\right)_T + \frac{\pi}{\hbar} \sum_{p,p'} n_T(p) \times \left|\langle m, p' | \underset{\approx}{T} | m, p\rangle - \langle 0, p' | \underset{\approx}{T} | 0, p\rangle\right|^2 \delta(E_p - E_{p'}) \quad , \tag{40}$$

involved and the $T_1$ terms have a temperature dependence similar to $T_2$ terms. This expression which contains the T matrix and the phonon temperature function, n, brings a subtle point about the dephasing of $|m\rangle$ states by phonons p, p'. If the two levels pumped by the laser have the same scattering amplitude, no loss of coherence is expected by any phase interruption mechanisms; only the spontaneous decay will destroy the correlation of the excited ensemble. This implies that electronic dephasing will be faster than IR dephasing and that pure singlet states might have different dephasing rates from those of pure triplet states.

To relate the dephasing of these TME to the original BO states, one uses equation (40) and the properties of $\mathcal{R}_{f'i'\,fi}$ between the final and initial states. For example, armed by equation (40) and using equations (37) and (39), one concludes that the intermolecular $T_1$ dephasing rate is:[20]

$$\left(\frac{1}{T_1}\right)^m_{TME} = \left(\frac{1}{T_1}\right)^s_{BO} \frac{v^2_{s\ell}}{(E_m - E_s)^2 + (\pi v^2_{s\ell}\rho_i)^2 + v^2_{s\ell}} \quad . \tag{41}$$

Equation (41) which contains the intramolecular density of states $\rho_i$, gives a Lorentzian distribution for the decay of TME. It is interesting to note that the radiative decay of TME also scales by the same mechanism [see equation (38)]. Similarly, one obtains expressions for $T_2$, which contain the cross terms of $\alpha$ and $\beta$.

The preparation of the BO state by broad band excitation[18] results in an additional channel for the loss of optical coherence. This is because

$$\left|\langle s|G_m(t)|s\rangle\right|^2 = \left|\sum_m |\langle m|s\rangle|^2 e^{-iE_m t/\hbar}\right|^2 \tag{42}$$

where G is the molecular propagator; $e^{-i\mathcal{H}_m t/\hbar}$. At short times the Fourier integral will therefore give:

$$\left|\langle s|G_m(t)|s\rangle\right|^2 = e^{-\frac{2\pi}{\hbar} v^2_{s\ell}\rho_i t} \tag{43}$$

which is the intramolecular decay that destroys the phase coherence of the BO state that is in quasi-resonance with many states. At longer time the system decays by the radiative lifetime of the state and exhibits oscillations when considering the radiation field in, and the Fourier sum of equation (42). Note that the oscillations depend on the phase angle between $|m\rangle$ and $|m'\rangle$ states. The conclusion of this section indicates therefore that the narrow and wide band excitation of molecules in condensed phases[18] and in beams[6] may help us in identifying the different dephasing processes described above.

Bulb vs Beam Experiments

In the bulb, collisional relaxation ensures that the system reaches equilibrium at long times. This means that the coherent excitation can be described by Bloch equations of a closed two-level ensemble. The method described here for the detection of coherence on the spontaneous emission monitors two sub-ensembles, $\alpha$ and $\beta$; those which are on-resonance with the laser field, i.e., $\omega = \omega_0$, and those which are off-resonance, i.e., $\omega - \omega_0 > 1/T_2$. The solution of the density matrix gives, therefore, the following emission intensity at any time t and into any vibrational level v:

$$I_v(t) = -\tfrac{1}{2} \frac{T_1 T_2 (\mu \cdot \mathcal{E}/\hbar)^2 (T^{(r)}_{1v})^{-1}}{[1 + T_1 T_2 (\mu \cdot \mathcal{E}/\hbar)^2]} \left[\left(\cos \bar{\Omega} t + \frac{\sin \bar{\Omega} t}{\bar{\Omega} T}\right) e^{-t/T} - e^{-t/T_1} - 1\right]$$

$$\bar{\Omega} = \left[(\mu \cdot \mathcal{E}/\hbar)^2 - \tfrac{1}{4}\left(\frac{1}{T_1} - \frac{1}{T_2}\right)^2\right]^{\frac{1}{2}} \qquad \frac{1}{T} = \tfrac{1}{2}\left(\frac{1}{T_1} + \frac{1}{T_2}\right) \tag{44}$$

which indicates that in addition to the usual $T_1$ decay, one expects the emission to exhibit a damped oscillatory function with a frequency $\bar{\Omega}$, on resonance. Therefore, as the laser is switched between different packets, one expects to see population build-up in the $\alpha$-packet and decay in the $\beta$-packet, together with beats. This expression is derived for the cases where the lower state relaxes with the same $1/T_1$ rate as the excited state.

Two distinct kinds of beats are expected on the decay of molecules. The first kind is a genuine intramolecular beating among the molecular levels. As discussed, before, this is expected in large molecules when the laser excitation prepares the BO state. The second kind of coherent oscillation on the emission is due to the optical nutation of a homogeneous packet, as discussed above.

Figure 3 depicts the decay of iodine gas in a bulb at 12 mtorr. Shown in this figure is the computer fit for all the data points. The match is excellent and gives $T_1 = 1.20 \pm 0.02$ $\mu$sec. The decay is due to the molecular eigenstates which have the Rabi frequency of equation (38). It is also different from the decay that has Zeeman quantum beats due to hyperfine coupling.[21] The insert in this figure shows the beats seen at short times in the decay together with the computer plot for the theoretical curve. The procedure is as follows. The entire experimental curve was fed into the computer to give the best $T_1$ fit. The computer then subtracted the $T_1$ curve from the experimental points to give the best pattern shown in the insert. This pattern gives both the decay of the coherent oscillations and the beating frequency: $\bar{\Omega} = 16.5 \pm 1.5$ MHz and $T = 0.44 \pm 0.06$ $\mu$sec. These results, when compared with the dephasing time (0.55 $\mu$sec) obtained from the photon echo experiments discussed later, indicate that the decay is not totally due to dephasing[22] and that the oscillation frequency is in excellent agreement with that of the nutation observed in the forward direction at the same laser power density. Moreover, these oscillations describe the true molecular eigenstates and are not due to intramolecular radiationless processes.

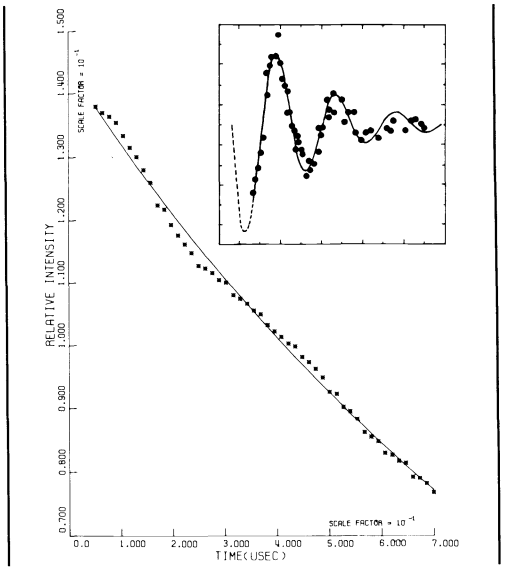


Fig. 3. The observed IRD signal (at short times) for $I_2$ at 12 mtorr. The solid line is the least squares fit for the observed decay. The single mode laser power at 5897.5 Å was 35 mw and the electro-optic switching frequency was 18 MHz. Insert: An enlarged view of the difference spectrum obtained by computer subtraction of the actual data points from the corresponding computer fit ($T_1$) values. The oscillation frequency is 16.5 ± 1.5 MHz and the damping time is 0.44 ± 0.06 $\mu$sec.

The incoherent resonance decay (IRD) which gives the optical $T_1$ in the bulb is analyzed at different pressures. The results show that

$$\frac{1}{T_1}\ (\mu\text{sec}^{-1}) = (0.775 \pm 0.029) + (0.0158 \pm 0.0004)P \tag{45}$$

where P is in millitorr. Two observations can be made from these results. First, the natural radiative decay time of the selectively excited state is 1.29 ± 0.05 $\mu$sec which gives a homogeneous linewidth of 123 ± 5 KHz. Secondly, the quenching cross section for the pressure induced broadening is $\sigma = 70 \pm 2$ Å$^2$. Knowing the exact radiative lifetime from the Stern-Volmer plot and the beam experiments, we concluded that Q′ (specific quenching rate times the radiation lifetime) is $3.6 \times 10^5$ liters/mole. This means that the collision efficiency is 1.1 considering the long-range energy correction to the hard sphere cross section of the Lennard-Jones potential.

In the beam the situation is different. One must consider the feeding[23] into the ground state as well as the transit time for the molecules in the laser beam. The transient following the electro-optic switching of the laser out of the transition frequency of the iodine beam is shown in Figure 4. The IRD signal is not seen when the switching frequency is below 0.3 MHz which is close to the width of the homogeneous resonance. Figure 4 also depicts the absence of the signal when the laser is off-resonance. The on- and off-resonance conditions are also checked by observing the emission of $I_2$ in the bulb.

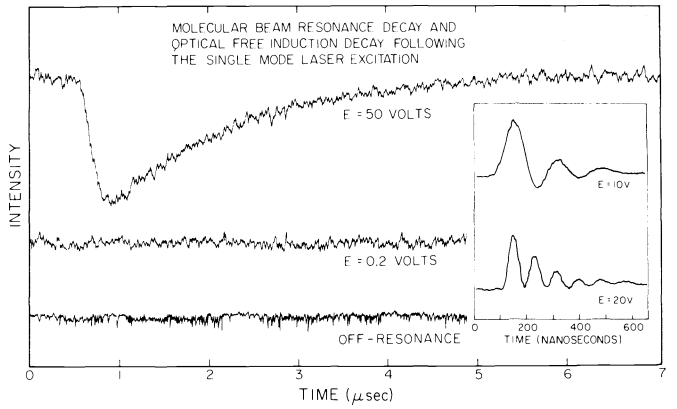


Fig. 4. The resonance decay and optical free induction decay of the coherently excited $I_2$ beam. The top two traces were taken with an electro-optic voltage of 50 and 0.2. The bottom trace was taken when the laser was off-resonance with the beam. The background pressure during all these measurements was $3 \times 10^{-6}$ torr. The insert in this figure shows the optical free induction decay signal. As expected, the beat signals which disappear in the absence of $I_2$ follow the electro-optic switching frequency. Of course, the signal disappears when the laser is blocked. The least squares fitting of all the data points gave a single exponential whose time constant is determined by $T_2$ and the Rabi frequency. The Rabi frequency in the beam was computed by measuring the nutation frequency of the bulb and scaling it by the square root of the power density ratio (beam-to-bulb).[23]

Since $\mu \cdot \mathcal{E}$ (laser power is up to 100 mwatts) is much larger than $T_2^{-1}$, a fast build up is expected for the absorption which reaches the saturation limit, and a decay determined by $T_1$. The coherent oscillation seen on the IRD of clean iodine samples is not observed in the beam because the depth of these oscillations is very small due to the power and transit time averaging. As in the optical nutation,[24] the averaging of the beam I(t) equation must be taken into consideration.[6, 23] It should be noted, however, that even in the presence of the oscillations, the overall decay will still give $T_1$. We, therefore, conclude that for $I_2$ in a collisionless beam $T_1 = 1.24 \pm 0.02$ μsec. These results show that (a) the beam decay is in excellent agreement with the zero-pressure value of $I_2$ in the bulb; and (b) the IRD of the beam is different from the decay following the 5145 Å excitation done by Ezekiel and Weiss.[25] The reported lifetime is $3 \pm 0.5$ μsec. These differences in lifetimes are due to iodine dissociation whose probability does not change monotonically as the rovibronic energy increases. Finally, the natural width of the selectively excited $X\ ^1\Sigma_g^+ \rightarrow B\ ^3\Pi_{0^+u}$ rovibronic state at 5897.5 Å is 128 ± 2 KHz.

The bulb result which is in agreement with the beam IRD result gives a nonradiative quenching similar to previous emission measurements[26] which utilize broad band excitation. Thus the influence of state preparation, on $T_1$ decay encountered in large molecules,[18] is not important. The results, however, give a cross section that is different from those measured by absorption techniques.[8] It was pointed out before[8] that this difference is because inelastic processes between the pumped level and neighboring levels will not necessarily produce a nonradiative decay into the ground state. In other words, the IRD gives the overall nonradiative cross section of the excited state population to the ground state. However, recent calculations[27] have yielded a cross section of 64 $Å^2$ for cross relaxation and phase shifts. This value is in reasonable agreement with our results.

To obtain the optical dephasing in the beam, the forward coherent signal which rides on top of the laser was detected. This way we observed the optical free induction decay in the iodine beam following the coherent excitation by the laser. The heterodyne signal which shows beats between the emitted light and the switched laser frequency is depicted in Figure 4. The results demonstrate that coherent optical transients in molecular beams can be observed even if the density is low. The beat frequency follows the electro-optical switching frequency while the decay is consistent with the conclusion that $2T_1 \approx T_2$ in the collisionless beam, considering the above mentioned approximations. This is an important conclusion because it says that in molecules like iodine there are essentially no intramolecular relaxations that destroy the phase coherence, and that the spontaneous loss is responsible for the optical dephasing at zero pressure. In large molecules (e.g., pentacene) and in molecules like $NO_2$, where intramolecular decay processes

may occur, the optical dephasing in the beam should not necessarily relate to $T_1$ at zero pressure. The experiments on these systems should be feasible since we already know[9] that optical nutation can be observed.

The above measurement of optical $T_2$ from FID suffers from power saturation effects since the decay of the signal depends on the averaging over the inhomogeneous broadening of the transition spanned by the laser. Our technique[10] of the right-angle photon echo eliminates this problem completely and monitors the total dephasing process on the emission into different vibrational-rotational levels of the molecule. The theory is already discussed and in what follows we present the results.

Figure 5 depicts the spontaneously detected photon echo in iodine as the probe pulse is swept through the echo position at $\tau_1 = \tau_2 = 180$ nsec. At longer time $\tau$ and large switching frequency, up to eight oscillations have been observed on the echo profile. The decay of the echo follows $e^{-2\tau/T_2}$ (see Figure 5) and at 10 mtorr gas pressure we found that $T_2 = 500 \pm 50$ nsec. The decay of the "forward" echo gives $T_2$ which is in agreement with previous work[8] and with the probe pulse results.[10]

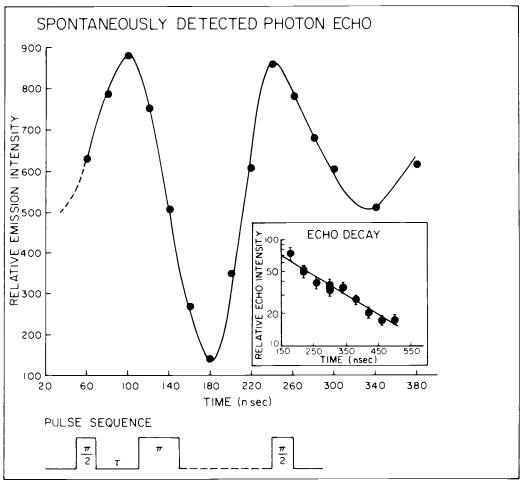


Fig. 5. The right-angle photon echo in iodine at 10 mtorr pressure using a three-pulse sequence. Here, $\tau_1 = 180$ nsec and $\tau_2$ was scanned to locate the echo. Note the maximum amplitude is at $\tau_2 = 180$ nsec where the photon echo appears as emission loss. The insert is a least squares fit of the amplitude of the photon echo (at $\tau_1 = \tau_2$) as a function of pulse separation.

Using one pulse the IRD gives $T_1 = 1.08$ $\mu$sec at 10 mtorr for the transition. The molecular beam and bulb results indicate that in the collisionless regime $T_1 = 1.24$ $\mu$sec. Since the ground state radiative decay rate is essential zero, the echo decay indicates that the radiative and nonradiative broadenings of the homogeneous resonance ($X\,^1\Sigma_g^+ \rightarrow B\,^3\Pi_{0^+u}$) in iodine are 128 KHz and 451 KHz, respectively. This total homogeneous width of 579 KHz is much smaller than the Ca. 400 MHz inhomogeneous width which corresponds to a dephasing time of 796 psec. Furthermore, if we assume that at this low pressure the excited state nonradiative decay due to quantum jumps into radiative levels is small and that the ground state nonradiative decay time is relatively long, one concludes that the broadenings due to pure dephasing and nonradiative processes are 368 KHz and 83 KHz, respectively. This means that 64% of the width is due to dephasing. Note that the echo measurements of $T_2$ should not be sensitive to effects due to power broadening as in cw frequency scanning techniques. The overall elastic scattering which leads to phase interruptions is determined by the microscopic anisotropy of the scattering events in the ground and excited states. On the other hand, the inelastic loss is due to collision-induced radiationless deactivation. As expected, therefore, the echo amplitude must change when the gas pressure increases, as confirmed experimentally by the three-pulse echo. These experiments are now being extended in our laboratory to nozzle and effusive beams in a variety of systems (e.g., $NO_2$ and pentacene) in order to examine the nature of optical dephasing at zero pressure.

## Condensed Phase Experiments

Molecules in solid matrices (e.g., mixed crystals) are called "isolated" from the host influences. However, phonons play an important role in the dephasing process and it is, therefore, important to separate intra- and intermolecular relaxation processes. The system we studied is pentacene in p-terphenyl at low temperatures (1.7 K and above). Using this system we have reported recently on the first observation of optical nutation in solids.[28] Subsequently, the FID in this system was observed by deVries et al.[29] The photon echo of this system using broad band excitation was also reported last

year.[30] Figure 6 shows typical coherent transients observed in our laboratory.

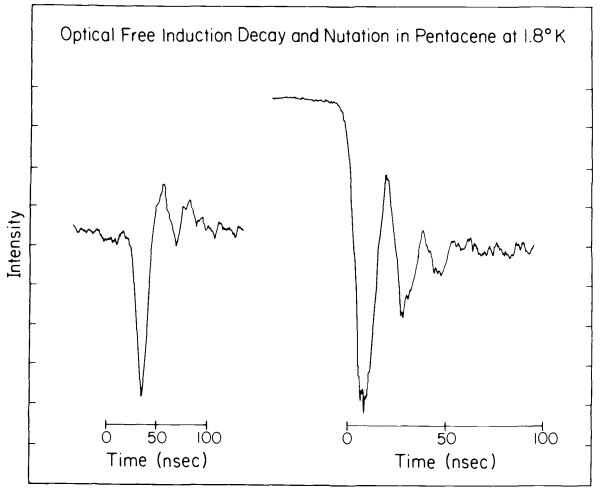


Fig. 6. Optical nutation (left) and optical free induction decay (right) of pentacene in p-terphenyl at 1.8 K.

The vibronic structure in a large molecule-like pentacene with 102 optical modes belongs to the statistical limit where the density of vibrationally hot ground states in the neighborhood of $\phi_S$ is very large. However, pentacene is known to have nearby BO triplet states. Moreover, not all the modes of the $\{\ell\}$ states are active in the coupling because of the symmetry requirement and/or the Franck-Condon overlap. Therefore, the coupling between $\phi_S$ and the discrete $\{\ell\}$ levels will give rise to molecular eigenstates that have a resonance width determined by the strength of the coupling to the molecular continuum formed on the ground state and to the continuum of the radiation field. Narrow band excitation should therefore select these states while wide band excitation should prepare some packets that evolve in time differently. The $T_1$ decay in the narrow band excitation will reflect the relative amplitude of the singlet state in the molecular eigenstates. Excitation of a large number of $\psi_m$'s yields a short decay (like a dephasing decay process) and a long decay of essentially the state $\psi_m$, in addition to a complicated beat pattern which depends on the level structure [see equation (42)]. The amplitude ratio of the fast decay to long decay depends on the number of states involved in the coupling. This explains why it is sometimes not feasible to see the long decay in such experiments.

Figure 7 d and e depicts the observed signal of pentacene in p-terphenyl (1.7 K) by the electro-optic (EO) modulation method. Several observations[18, 31] were made: (1) the decay changes from ~ 15 $\mu$sec to ~25 nsec when the effective laser width changes from 6 MHz to 18 GHz; (2) at high temperatures, the signal disappears; (3) there is a magnetic field effect on the decay in the narrow band laser excitation; (4) the decay signal is absent when the molecule is excited above the 0, 0 electronic origin, and the emission is detected at the same d.c. level as that of the origin; (5) the decay time does not change when the power level of the laser is reduced in the range we studied; (6) the $T_1$ decay is exponential and changes as we scan the narrow-banded laser in the manifold of the first electronic origin; (7) the "narrow" band coherent transients give a $T_2$ of 45 nsec when the laser is on-resonance with the 0, 0 transition, but less than a few nanoseconds when the laser is in resonance with the vibronic line at 267 $cm^{-1}$ above the 0, 0 transition; (8) the signal gets larger at higher switching frequencies; and finally (9) the measurement of dephasing rate vs temperature shows a transition temperature for the loss of coherence; the system response is almost flat at low temperatures and undergoes the transition at $\approx$ 3.7 K. These observations forced us to conclude that the preparation of molecular eigenstates can be done if the laser width is narrow enough and the resonances are not smeared to form a continuum. On the other hand, the broad band excitation prepares packets which as mentioned before, decay by a fast dephasing component ($\sim v^2_{s\ell\rho}$) and a low amplitude slow-decay component. It should be mentioned that in pentacene low-pressure gas and at zero pressure, a transient spectrum[32] of hot excited levels in the neighborhood of $\phi_S$ was found when the system was excited by broad band excitation. The decay time (100 $\mu$ sec) becomes shorter at high pressures. However, EO methods monitor both the decay of the off-resonance molecules and the transient build-up of the newly excited molecules. To separate these effects we used an acousto-optic (AO) technique which we discuss in the following section.

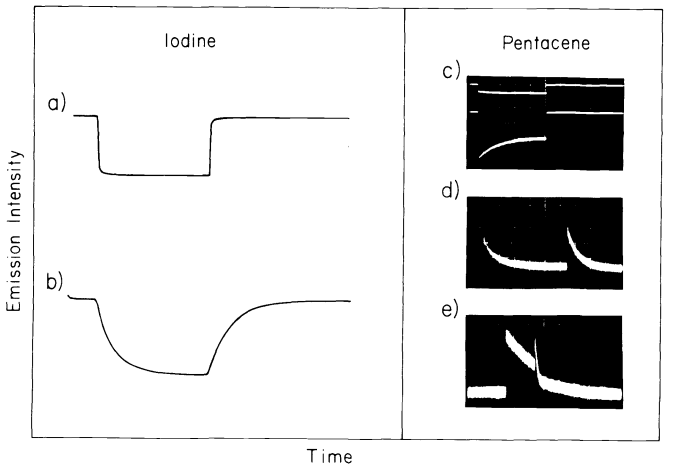


Fig. 7. The AO and EO laser modulation of iodine gas and pentacene in p-terphenyl at 1.8 K: a is the AO light pulse (width = 3.4 $\mu$sec) and b is the iodine response (raw data). Note the decay on the falling edge of the pulse and the build up on the leading edge. c is the AO signal from pentacene (10 $\mu$sec/div). d (20 $\mu$sec/div), and e (5 $\mu$sec/div) are the signals of pentacene when excited with long and short EO pulses, respectively. Note that in e on the leading edge the system is excited by a long pulse while on the falling edge the system is excited only by ~ 10 $\mu$sec pulse.

Recently our laboratory has completed optical coherence experiments on iodine and pentacene isolated in p-terphenyl using an acousto-optic technique to rapidly switch the single-mode dye laser on and off. The

technique involves focusing the output of the dye laser into a quartz crystal which has a thin film transducer bonded to it. Phonons injected by an RF oscillator create an acoustic wave in the crystal which diffracts up to 50% of the incident light at the Bragg angle. This diffracted beam, shifted in frequency by the acoustic phonon frequency is deflected into the sample for the duration of the RF pulse ($\pi/2$, $\pi$ or any length). Thus the acousto-optic modulator acts as a fast shutter. The characteristics of the laser pulse this technique provides are determined by (1) the RF pulse width and the rise/fall times, and (2) the transit time of the acoustic wave across the focused laser beam in the crystal. Before focusing the laser pulse on the sample it is passed through a Glan-Thompson polarizer to insure clean linear polarization. Analogous with the frequency switching experiments, the emission intensity from the sample is monitored at right angles to the exciting beam.

We tested this technique on an iodine transition previously studied by the frequency switching technique and found an emission lifetime (at 30 mtorr pressure) consistent with earlier results as shown in Fig. 7. However, when we tried this technique on pentacene in p-terphenyl our results were dramatically different from the frequency switching experiments.

Monitoring the emission from the lowest excited singlet state ($O_1$ site) while the laser was switched on and off, we found a decay pattern similar to that observed in our frequency switching experiments when the laser was <u>on</u> and a very rapid (~ 29 nsec) decay following the falling edge of the laser pulse (10 nsec decay time).

This result, in addition to all of the other experimental observations for this system reported earlier had led us to reevaluate the coupling scheme in the molecular eigenstate picture.

If the molecular eigenstates described earlier are of the form(37) and one assumes that the coupling provides one eigenstate, $\psi_{m*}$ that carries a large fraction of the oscillator strength of the transition (i.e., $\alpha_{ms*} \gg \alpha_{ms}$) then one can construct a model consistent with both the electro-optic and acousto-optic experimental observations.

This eigenstate decays rapidly by $\Gamma_{m*}$ since it is mostly singlet in character and slowly communicates ($V_{mm*}$) with the other molecular eigenstates providing a nonradiative pathway ($\Gamma_m$) to the ground state.

The time evolution of the population of $\psi_{m*}$ will give us the emission dynamics of the frequency switching experiments. Considering a group of molecules brought into resonance with the level structure described above one can show that the population of $\psi_{m*}$ and thus the emission intensity is

$$P^{r}_{m*}(t) = \frac{K_p}{\lambda^+ - \lambda^-}\left[\left\{\frac{\bar{\Gamma}_m + P_0(0)\lambda^+}{\lambda^+}\right\} e^{\lambda^+ t} - \left\{\frac{\bar{\Gamma}_m + P_0(0)\lambda^-}{\lambda^-}\right\} e^{\lambda^- t}\right] + \frac{K_p \bar{\Gamma}_m}{\lambda^+\lambda^-} \qquad (46)$$

where r refers to a group on resonance, $K_p$ is the pumping rate, $\bar{\Gamma}_m$ is the average lifetime of the weakly coupled eigenstates, $P_0$ is the population of the ground state and

$$\lambda\pm = -\tfrac{1}{2}(2K_p + \bar{\Gamma}_m + \Gamma_{m*}) \pm \tfrac{1}{2}\sqrt{(2K_p - \bar{\Gamma}_m + \Gamma_{m*}) - 4K_p V_{mm*}} \quad . \qquad (47)$$

However, in the frequency switching experiments we must consider the contribution to the observed emission intensity of two groups of molecules; those originally on resonance (a), and those switched into resonance (b). Thus, for a complete description we need the off-resonance (or) solution for the time evolution of $\psi_{m*}$. This is easily shown to be

$$P^{or}_{m*}(t) = P_{m*}(0)\, e^{-\Gamma_{m*} t} \quad . \qquad (48)$$

With appropriate boundary conditions one can now determine the IRD emission dynamics in the frequency switching experiments at all times. Initially on resonance with group a we have simply to consider equation (46). When the laser frequency is switched into resonance with group b we then have for the total emission intensity

$$I(t) = P^{a,\,or}_{m*}(t) + P^{b,\,r}_{m*}(t) \quad . \qquad (49)$$

Equation (49) also holds (with resonance and off-resonance conditions for groups a and b reversed) when the laser frequency is switched back. By examining the form of equation (46) one can see that if the pumping rate is not significantly greater than the lifetime $\Gamma_{m*}$ then there will be a smooth build-up in the IRD emission intensity as the laser is switched resulting from the difference between the increase in emission due to group b and the decrease in emission due to group a followed by a slow decay to an equilibrium condition (see Fig. 7).

In the acousto-optic shutter experiments equation (46) holds during the laser pulse while equation (48) applies when the pulse is switched off. Since no long component is observed in the (AO) experiments when the laser is shut off we must conclude that the weakly coupled molecular eigenstates decay primarily nonradiatively (by $\Gamma_m$) back to the ground state.

This mechanism can fit both the observed decay pattern in the frequency switching experiments as well as the acousto-optic shutter experiments and we are now studying the system as a function of laser pulse width (in both cases) to understand further the effect of pulse width on state preparation.

It should be mentioned at this point that an equivalent mechanism involves the preparation of a singlet state which intersystem crosses to the triplet manifold. Molecular beam experiments should allow one to decide which mechanism is appropriate since in a collisionless molecular beam, communication (by spontaneous emission of phonons) between eigenstates is not possible and so one would not see the long decay during the laser pulse while intersystem crossing can indeed occur and the long decay should still be present. This beam experiment is now in progress.

## Epilogue

The experiments discussed in this paper have focused on the disentangling of the inhomogeneous resonance transitions in gases, solids and molecular beams. The importance of these experiments lies in their provision of direct information on the optical dephasing processes that take place within the molecule and in the ensemble. However, this is just the beginning. Indeed, many more experiments are needed. We take this opportunity to mention a few of these experiments that are already started in our laboratory.

We are currently studying $NO_2$ in bulbs and in beams. The objective is to resolve the anomaly found by Zare in his recent experiments of the Hanle effect. Zare's group[33] and Demtröder et al.[34] have found that the homogeneous linewidth at zero pressure does not equal the width expected from the spontaneous lifetime for well-behaved state g-factor. We have shown before that optical nutation can be observed in $NO_2$. Therefore, direct measurements of optical $T_2$ and $T_1$ using the techniques mentioned in this paper will resolve this dilemma, and tell us whether or not intramolecular processes are operative at zero pressure. To understand the transient signals in $NO_2$ (and also in pentacene) one must consider the velocity distribution in the beam, the ground state feeding and the transit time of the molecules in the laser beam. The complete solution[23] for the density matrix for molecules in a laser beam is shown in Figure 8. The calculation included the effect of velocity inhomogeneity, the detector geometry and the beam temperature and is different from the unphysical analysis given by Allen et al.[35] We conclude from our work that special care should be given to the analysis of transients in the beam and that the bulb analysis is not applicable.

Finally, these coherent optical techniques are now being extended to the sub-picosecond region using our laser (pulse width = 0.6 psec, and transform limited) which operates on the principles of mode-locked dye lasers.[36, 37] This way we hope to learn about dephasing at higher temperatures in solids or higher pressures in gases, and to hopefully probe the "ergodic" behavior of molecules in gases, solids, and beams.

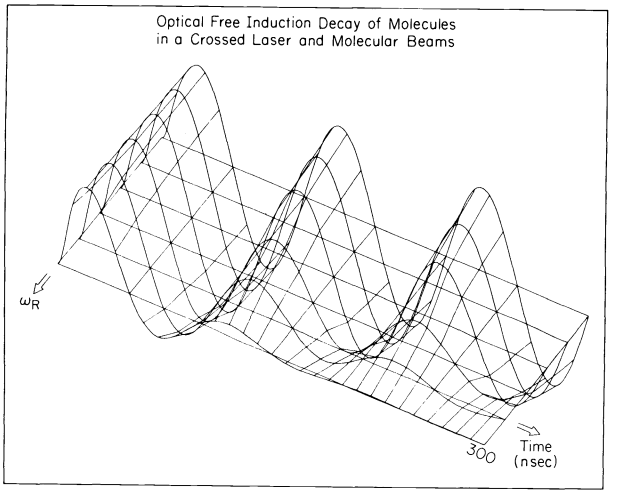


Fig. 8. Optical free induction decay in pentacene beam. The Rabi frequency is varied from 0.3 to 20 MHz. The beats seen in this figure are due to the heterodyne detection scheme. Note that the decay gets faster as $(\mu \cdot \mathcal{E}/\hbar)$ gets larger, but different from the bulb results.

## Acknowledgments

This work is supported in part by the Research Corporation and the United States Energy Research and Development Administration. Acknowledgment is also made to the donors of the Petroleum Research Fund, administered by the ACS, for partial support of this research. This work is Contribution No. 5676.

## References

1. Weisskiop, W. and Wigner, E., Z. Physik, 63, 54 (1930).
2. See, e.g., Sargent III, M., Scully, M. and Lamb, Jr., W. E., Laser Physics, Addison-Wesley Publishing Company, 1974.
3. Dicke, R. H., Phys. Rev., 93, 99 (1954).
4. Feynman, R. P., Vernon, Jr., F. L. and Hellworth, R. W., J. Appl. Phys., 28, 49 (1957).
5. Abragam, A. The Principles of Nuclear Magnetism, Oxford University Press, London, 1961.
6. Zewail, A. H., Orlowski, T. E., Shah, R. R. and Jones, K. E., Chem. Phys. Lett., 49, 520 (1977) and references cited therein.
7. Kurnit, N. A., Abella, I. D. and Hartmann, S. R., Phys. Rev. Lett., 13, 567 (1964).
8. Brewer, R. G., Science, 178, 247 (1972) and references therein; Brewer, R. G. and Genack, A., Phys. Rev. Lett., 36, 959 (1976).
9. Zewail, A. H., Orlowski, T. E. and Dawson, D. R., Chem. Phys. Lett., 44, 379 (1976); Orlowski, T. E., Jones, K. E. and Zewail, A. H., Chem. Phys. Lett., 50, 45 (1977).
10. Zewail, A. H., Orlowski, T. E., Jones, K. E. and Godar, D. E., Chem. Phys. Lett., 48, 256 (1977).
11. Godar, D. E. and Zewail, A. H., to be published.
12. Telle, J. and Tang, C. L., Appl. Phys. Lett., 24, 85 (1974); ibid., 26, 572 (1975).
13. By a BO state we mean the state which carries most of the oscillator strength. This is because a real BO state might not exist and that the state we excite is a mixture of BO states. However, this terminology is known among the researchers in this field and does not in any way influence the conclusions of our discussion here. We have benefited from the stimulating discussions with G. W. Robinson of Texas Tech regarding this point about the preparation of "pure" BO states.
14. Jortner, J. and Mukamel, S. in: The World of Quantum Chemistry, eds. R. Dandel and B. Pullman, Deidel Publishing Company, Boston, 1974; Freed, K. F., Topics in Appl. Phys., 15, 23 (1976).
15. Bixon, M. and Jortner, J., J. Chem. Phys., 50, 4061 (1969).
16. Rhodes, W., Henry, B. R. and Kasha, M., Proc. Natl. Acad. Sci. (USA) 63 31 (1969); Delory, J. M. and Tric, C., Chem. Phys., 3, 54 (1974); Mukamel, S. and Jortner, J., in: Excited States, Vol. 3, Academic Press, New York, 1977, in press; Langhoff, C. A. and Robinson, G. W., Mol. Phys., 26, 249 (1973); Langhoff, C. A., Chem. Phys., 20, 357 (1977).
17. Redfield, A. G., Adv. Mag. Res., 1, 1 (1965).
18. Zewail, A. H., Orlowski, T. E. and Jones, K. E., Proc. Natl. Acad. Sci. (USA) 74, 1310 (1977); ibid., Spec. Lett., 10, 115 (1977).
19. Liu, W.-K. and Marcus, R. A., J. Chem. Phys., 63, 272 (1975).
20. In deriving this equation, we have assumed equal level spacing and that the phonon-induced relaxation in the triplet manifold is slower than in the singlet. This is because the energy gap between the excited singlet and triplet states is much smaller than the excitation energy. With this sparse level structure, phonons with a certain frequency spectrum are needed in order to open the vibrational relaxation channels. This, of course, might not be the case in many systems, nevertheless, equations (40) and (41) point out that the relationship between $T_1$ and $T_2$ of the BO and TME states can be obtained using this formalism.
21. Wallenstein, R., Paisner, J. A. and Schawlow, A. L., Phys. Rev. Lett., 32, 1333 (1974).
22. In reference (6) we pointed out the reason behind the mismatch between the value of this decay and that of $\frac{1}{2}(1/T_1 + 1/T_2)$. Basically, the inhomogeneity of the laser and the Doppler averaging are the sources of the "inhomogeneous" decay which is faster than the intrinsic decay of the coherently excited two level system.
23. Jones, K. E., Nichols, A. and Zewail, A. H., to be published.
24. Tang, L. G. and Silverman, B. D., Physics of Quantum Electronics, eds. P. Kelley, B. Lax, and P. Tannenwald, McGraw-Hill, New York, p. 280, 1966; Shoemaker, R. L. and van Stryland, E. W., J. Chem. Phys., 64, 1733 (1976).
25. Ryan, T. J., Youmans, D. G., Hackel, L. A. and Ezekiel, S., Appl. Phys. Lett., 21, 320 (1972); Ezekiel, S. and Weiss, R., Phys. Rev. Lett., 20, 91 (1968).
26. Capelle, G. A. and Broida, H. P., J. Chem. Phys., 58, 4212 (1973); Steinfeld, J. I. and Schweid, A. N., J. Chem. Phys., 53, 3304 (1970); Brown, R. and Klemperer, W., J. Chem. Phys., 41, 3072 (1965); ibid., 42 3475 (1965); Kurzel, R. B. and Steinfeld, J. O., J. Chem. Phys., 53, 3293 (1970); ibid., 44, 2740 (1966); Chutjian, A., Link, J. K. and Brewer, L., J. Chem. Phys., 46, 2666 (1967).
27. Mukamel, S., Reuven, A. B. and Jortner, J., J. Chem. Phys., 64, 3971 (1976).
28. Zewail, A. H. and Orlowski, T. E., Chem. Phys. Lett., 45, 399 (1977) and reference 9.
29. de Vries, H. and Wiersma, D. A., to be published.
30. Aartsma, T. and Wiersma, D. A., Phys. Rev. Lett., 36, 1360 (1976).
31. Orlowski, T. E., Jones, K. E. and Zewail, A. H., to be published.
32. Soep, B., Chem. Phys. Lett., 33, 108 (1975); Sander, R. K., Soep, B. and Zare, R. N., J. Chem. Phys., 64, 1242 (1976).
33. Zare, R., private communication.
34. Paech, F., Schmiedl, R. and Demtröder, private communication.
35. Allen, L., Allen, B. and Knight, P. L., Optics Comm., 20, 150 (1977).
36. Shank, C. V. and Ippen, E. P., Appl. Phys. Lett., 24, 373 (1974).
37. Ruddock, I. S., and Bradley, D. J., Appl. Phys. Lett., 29, 296 (1976).